

PETROGRAPHY OF THE KINGSTON EXPERIMENTAL SIDEWALK AT AGE 22 YEARS – ASR AS THE CAUSE OF DELETERIOUSLY EXPANSIVE, SO-CALLED ALKALI-CARBONATE REACTION

Tetsuya Katayama ^{1*}, Patrick E Grattan-Bellew ²

¹Kawasaki Geological Engineering Co. Ltd., Tokyo, Japan

²Materials & Petrographic Research G-B Inc.

Abstract

Detailed SEM-EDS analysis of the Kingston sidewalk concretes in Canada revealed that ASR is responsible for expansion of so-called ACR, producing ASR gel that fits general trends of typical ASR gel on the [Ca/Si]-[Ca]/[Na+K] diagram. Dedolomitization gave no evidence of expansion but caused carbonation of ASR gel leaving a fragile texture, masking petrographic evidence of ASR in optical microscopy. The same applies to a concrete failure in Kentucky, USA, where high-Ca fly ash and low-alkali Portland cement could not suppress ASR of chert and dolomitic limestone aggregates. High-alumina cement was found to produce expansion by ASR and dedolomitization.

Keywords: alkali-carbonate reaction, ASR gel, dedolomitization, EDS analysis, minimum cement alkali

1 INTRODUCTION

The Kingston experimental concrete sidewalk, now demolished, was placed by the Ontario Ministry of Transportation in 1985 to investigate alkali-carbonate reaction (ACR) of the Pittsburg aggregate in Kingston, Ontario, Canada [1]. In 2007, core samples were taken for a petrographic study and the first result was published in 2008 [2,3]. Because previous concrete samples of ACR studied by the first author were old, more or less affected by weathering and leaching [4-6], it was necessary to investigate freshly taken core samples to exclude such secondary factors. As a result, detailed petrographic examination was jointly made of fresh samples to draw a definitive conclusion about the so-called ACR, including similar deterioration which is occurring in Kentucky, USA.

2 MATERIALS AND METHODS

Core samples were extracted from three cracked sections of the Kingston sidewalk (Table 1), i.e. low-alkali (L), high-alkali (H), and high-alkali boosted (Na), the last one examined by Grattan-Bellew et al. [2,3] and also taken for a blind control (Nb). The Kentucky concrete came from a 5-6 year-old building (A, B). Concrete prisms with the Pittsburg aggregate (38°C, 100% humidity, 450 days), with ordinary Portland cement and high-alumina cement, respectively, were examined, along with concrete microbars (80°C, 1M NaOH, 28 days) with the most reactive layer of the Pittsburg quarry, with and without a Japanese blastfurnace slag (50%). Polarizing microscopy, SEM and quantitative EDS analysis (JEOL JSM 5310LV/JED 2140: 15KV, 0.12nA) were done on the same polished thin section (30mm by 20mm, 15µm thickness) to identify reaction products and analyze compositions of Portland cement phases (Table 2) [3]. Details of analytical conditions are given in [5]

* Correspondence to: katayamat@kge.co.jp

3 RESULTS

3.1 Cement phases and estimation of minimum alkali content

Unhydrated cement particles in concretes were analyzed by EDS for chemical compositions of major Portland cement phases (alite, belite, aluminate and ferrite). Good stoichiometry of atomic numbers was noted (Table 2). High-alkali concrete specimens from Kingston (N) contained elongated alkali aluminate, while low-alkali concrete (L) contained both alkali-aluminate and low-alkali cubic aluminate. The estimated minimum alkali content of the clinker (Table 1), based on compositions by EDS (Table 2), omits water-soluble alkali from alkali-sulfates that are no longer present in concretes. Conversion factors to estimate the alkali content of the cement were obtained by comparing the record and analytical data: e.g. $\times 1.16$ ($1.04/0.90$)- 1.37 ($1.04/0.76$) for high-alkali cements (H, Na, Nb); $\times 1.06$ ($0.56/0.53$) for low-alkali cement (L). Cement clinker in the Kentucky concretes (A, B) was low-alkali, hence the cement used would be correspondingly low-alkali, with $\text{Na}_2\text{O}_{\text{eq}}$ of around 0.5%.

3.2 Compositional trend lines of reaction products

On the $[\text{Ca}/\text{Si}]-[\text{Ca}]/[\text{Na}+\text{K}]$ diagrams (Figure 1) are shown the compositional trend lines of ASR gel analyzed by EDS in ACR-affected concretes. Alkali-boosted concrete of the Kingston sidewalk made from the same high-alkali cement, both open and blind samples (Figure 1, Na, Nb), presented typical ASR gel with a deflected line indicative of the *type III evolution* after Katayama [7], with narrower distribution. By contrast, low-alkali concrete (Figure 1, L) showed the *type I evolution* with a single line of wider distribution.

Kentucky concrete gave parallel trend lines of ASR gel of the *type II evolution* (Figure 1, A). The main longer line connects with the CSH gel (hydrates of alite and belite) at a “convergent point” around $[\text{Ca}/\text{Si}]=1.5$, $[\text{Ca}]/[\text{Na}+\text{K}]=100$. The slope of the alite hydration grades from negative with high-alkali cement (Figure 1, Na, Nb) through vertical (Figure 1, L) to positive with low-alkali cement (Figure 1, A).

3.3 Reaction products in field concretes

Kingston sidewalk

In the alkali-boosted section (Table 3, Na, Nb), a whole spectrum of petrographic features of deterioration can be seen, ranging from 1) rim formation (Figure 2a) through 2) internal cracking of aggregate (Figure 2b) to 3) crack extension into cement paste (Figure 2c), and further 4) gel deposition within air voids along cracks (Figures 2d,e). ASR gel lining cracks in the dolomitic aggregate was identified by SEM observation on the polished thin section (Figures 2f,g,h). Platy crystals of Friedel's salt, which reflects splash of deicing salt in winter, were found within air voids surrounded by a calcite lining. Similar tendency was also noticeable in the high-alkali section (Table 3, H) and in the low-alkali section (Figures 4a,b), but gel-filled voids were lacking in the latter.

Kentucky concretes

Dolomitic limestone coarse aggregate presented 1) dedolomitization rim (Figure 3a), 2) internal crack of aggregate, and 3) crack extending into the cement paste (Figure 3c). Under the SEM, cracks from pools of ASR gel in the dolomitic aggregate (Figure 3d) widened toward the cement paste, being filled with ASR gel (Figure 3e), which are carbonated and wearing out in the grinding processes of thin section preparation. Along the cracks formed by ASR, brucite presented pseudomorphs surrounding dolomite rhombohedra (Figure 3f). Chert particles in the sand also formed reaction rims and internal cracks filled with ASR gel (Figures 3g,h). Kentucky concretes contained abundant fly ash particles of high-Ca glass with $\text{CaO} > 35\%$, corresponding to class C fly ash (Figure 3b, Table 3).

3.4 Reaction products in laboratory concretes

Concrete prism

Ordinary Portland cement produced a large expansion (about 0.5%, 450 days) with abundant ASR gel and its carbonation (Figure 4c). Under the SEM, composite veins of ASR gel and porous calcite replacing the gel

(Figure 4d, Table 3), indistinguishable in optical microscopy, can be identified. By contrast, concrete prism with high alumina cement produced relatively small but deleterious expansion (0.08%, 450 days). Conspicuous dedolomitization rims (Figure 4e) appeared on the dolomitic aggregate particles, whereas radial expansion cracks were confined to the interior of the crushed dolomitic limestone and sand particles of mudstone and silty limestone. Dedolomitized rhombohedra (Figure 4f) had a rim with compositions resembling hydrotalcite (Table 3), rather than brucite. Cracks of the dolomitic aggregate contained ASR gel (Table 3) that was almost replaced by calcite vein (Figures 4g,h).

Concrete microbar

Cracking and ASR gel were evident (Figure 5a). Microcrystalline quartz in dolomitic limestone converted to ASR gel (Figure 5b) filling cracks open to the microbar surface. Crack-lining ASR gel is thinning out toward the interior of the aggregate (Figure 5c), and along the same crack, dolomite crystals underwent decomposition to rims (Figure 5d). Blastfurnace slag had some suppressing effect on the expansion of microbar until 14 days, but failed to prevent the formation of cracks filled with ASR gel at later ages (Figure 5e)(0.23%, 28days). ASR gel filled cracks in the cement paste (Figure 5f), running from the reacted dolomitic aggregate with dedolomitized rims (Figures 5g,h). In general, the alkali content of ASR gel was lower in the microbar made with slag than that without slag (Table 3).

4 DISCUSSION

Carbonation of ASR gel proceeds in dedolimitizing aggregate and forms a fragile mixture with calcium carbonate. Carbonate ions have two origins, i.e. dedolimitization and meteoric water seeping along cracks during exposure to the atmosphere and freeze/thaw cycles. This explains why crack-filling ASR gel has been missed in conventional petrography: 1) optically amorphous ASR gel overlapped by highly birefringent calcite is hidden in transmitted light, and 2) veins of carbonated ASR gel tend to wear off during sample preparation [5]. Thus, what we can see is not always what it is, nor what it is not. SEM-EDS analysis on the polished thin section enables this.

ASR gel in alkali-rich concrete is prone to carbonation and leaching alkalis. The evolutionary stage of ASR (Figure 1) was interpreted based on references [5,7,8]: the *type III evolution* of high-alkali concrete in Kingston, with a narrow range of ASR gel, suggests a high reaction rate and late stage of ASR. The low-alkali concrete from this sidewalk, with the *type I evolution* and a narrow range, indicates a moderate reaction and middle stage of ASR. The younger Kentucky concrete of low-alkali cement, presenting the *type II evolution*, indicates that ASR is at relatively early stage and slowly ongoing, because the main line occupies alkali-rich area. The negative slope of alite hydration in high-alkali cement (Figure 1, Na, Nb) is due to alkali release of alite into the cement paste, while the positive slope in low alkali cement (Figure 1, A) to the scarcity of alkali in alite and richness of alkali in cement paste.

The reason why the blastfurnace slag failed to prevent the formation of ASR gel and cracking in the concrete microbar at later age is because the crypto- to microcrystalline quartz present in an isolate form in the dolomitic aggregate was more reactive than slag particles, although slag had some effect of suppressing formation of expansive alkali-rich gel in concrete by absorbing alkali ions in its hydrates (Table 3). Both fly ash and low-alkali cement in the Kentucky concretes were ineffective in counteracting ASR of dolomitic aggregate and chert sand, because high-Ca fly ash glass has less pozzolanic reactivity than cryptocrystalline quartz. Generally, low-Ca fly ash glass with CaO <5 % is thought to be more reactive than high-Ca flyash glass, but this could not suppress ASR in field concrete in which aggregate was highly reactive bronzite andesite [8].

5 CONCLUSIONS

- ACR in the Kingston experimental sidewalk is a combined effect of harmless dedolomitization and deleteriously expansive ASR of cryptocrystalline quartz. Cracking proceeds like a typical ASR, i.e. rim-formation, internal cracking of aggregate, external cracking into cement paste and precipitation of ASR gel in air voids.
- Low alkali cement in the sidewalk concrete ($\text{Na}_2\text{O}_{\text{eq}} 1.74\text{kg}/\text{m}^3$) could not prevent the formation of radial expansion cracks filled with ASR gel, but dedolomitization was not related to the crack formation.

- Blastfurnace slag in concrete microbar (50% mix) modifies compositions of ASR gel to higher [Ca]/[Na+K], but it is not sufficient to suppress deleterious expansion of ASR in the long term.
- High-alumina cement in concrete prism is effective in mitigating expansion of ASR than ordinary Portland cement, but it is not sufficient to suppress it. Crack-filling ASR gel in the aggregate is prone to carbonation, but dedolomitization does not produce expansion crack, except for hydrotalcite rims on the dolomite rhombohedra.
- Concrete deterioration in Kentucky is also caused by ASR, not by dedolomitization. Combined use of low alkali cement and fly ash could not counteract ASR of dolomitic limestone coarse aggregate and chert in the sand, because fly ash glass was of high-Ca variety with low pozzolanic activity.

6 REFERENCES

- [1] Williams, DA and Rogers, C. (1991): Field trip guide to alkali-carbonate reaction in Kingston. Ontario Ministry of Transportation, Report MI-145: pp.26.
- [2] Grattan-Bellew, PE, Mitchell, LD, Margeson, J and Deng, M. (2008): Is ACR another variant of ASR? Comparison of acid insoluble residues of alkali-silica and alkali-carbonate reactive limestones and its significance for the ASR/ACR debate. Proceedings, 13th International Conference on Alkali-Aggregate Reaction in Concrete (ICAAR), Trondheim, Norway: 706-716.
- [3] Grattan-Bellew, PE, Mitchell, LD, Margeson, J and Deng, M.(2010): Is alkali-carbonate reaction just a variant of alkali-silica reaction ACR=ASR? Cement & Concrete Research (40): 556-562.
- [4] Katayama, T (2004): How to identify carbonate rock reactions in concrete. Materials Characterization (53): 85-104.
- [5] Katayama, T (2010a): The so-called alkali-carbonate reaction (ACR) - Its mineralogical and geochemical details, with special references to ASR. Cement & Concrete Research (40): 643-675.
- [6] Katayama, T (2011): So-called alkali-carbonate reaction - Petrographic details of field concretes in Ontario. Proceedings, 13th Euroseminar on Microscopy Applied to Building Materials (EMABM). Ljubljana, Slovenia: pp.15.
- [7] Katayama, T (2008): ASR gel in concrete subject to freeze-thaw cycles - Comparison between laboratory and field concrete from Newfoundland, Canada. Proceedings, 13th International Conference on Alkali-Aggregate Reaction in Concrete (ICAAR), Trondheim, Norway: 174-183.
- [8] Katayama, T (2010b): Diagnosis of alkali-aggregate reaction - Polarizing microscopy and SEM-EDS analysis. Proceedings of 6th International Conference on Concrete under Severe Conditions (CONSEC'10). Merida, Mexico, 19-34.

Alkalis in concrete			Kingston experimental sidewalk				Kentucky	
Record [1]	Concrete alkali (kg/m ³)	no. Na ₂ O _{eq}	H	L	Na	Nb	A	B
				3.22	1.74	3.88 *		
Estimation by EDS analysis	Alkali content of cement used (%)	Na ₂ O	0.62	0.34	0.62			
		K ₂ O	0.63	0.34	0.63			
		Na ₂ O _{eq}	1.04	0.56	1.04 *			
Estimation by EDS analysis	Minimum alkali content of clinker (%)	Na ₂ O	0.55	0.38	0.66	0.64	0.36	0.26
		K ₂ O	0.33	0.22	0.37	0.26	0.14	0.17
		Na ₂ O _{eq}	0.76	0.53	0.90	0.82	0.46	0.37

* alkali boosted to 1.25% of cement by the addition of NaOH, Na: uranyl coated [2,3], Nb: blind sample
 Assumed ratio of alite:belite: aluminate:ferrite (wt%) = 60:20:10:10 for nos. H, Na, Nb, A; 65:15:5:15 for nos. L, B (TABLE 2)

thin section particle	Alkali-boosted high-alkali concrete (Na)								Low-alkali concrete (L)							
	Alite		Belite		Aluminate		Ferrite		Alite		Belite		Aluminate		Ferrite	
	quen	ched	quen	ched	quen	ched	quen	ched	anne	aled	anne	aled	anne	aled	anne	aled
	4	4	4	4	4	4	4	4	3	2	3	2	3	2	3	2
A	B	A	B	A	B	A	B	B	A	A	A	C	B	C	B	
SiO ₂	24.84	25.01	31.74	32.83	6.73	7.75	4.51	4.58	24.28	24.96	31.82	32.69	5.61	5.83	4.76	1.59
TiO ₂	0.04	0.24	0.15	0.15	0.45	0.28	0.18	1.09	0.00	0.52	0.43	0.15	0.00	0.07	0.83	1.33
Al ₂ O ₃	0.59	0.72	1.22	0.58	23.15	23.00	19.63	15.61	0.77	0.51	1.36	0.58	22.62	26.92	19.55	15.24
Fe ₂ O ₃	0.36	0.47	2.06	0.37	10.54	7.15	25.03	24.95	1.13	0.14	1.10	0.95	10.86	5.61	22.39	34.06
MnO	0.27	0.00	0.00	0.24	0.00	0.00	0.00	0.72	0.35	0.39	0.30	0.00	0.00	0.44	0.01	0.00
MgO	1.14	1.11	0.48	0.00	1.23	0.65	3.55	2.75	0.47	0.95	0.84	0.30	2.22	0.85	2.51	0.97
CaO	68.79	69.59	59.65	61.07	49.67	51.26	45.29	45.98	70.16	67.12	60.16	63.04	51.61	57.56	46.78	44.65
Na ₂ O	0.43	0.14	0.62	0.35	3.22	3.91	0.58	0.12	0.10	0.36	0.85	0.56	2.39	1.04	0.29	0.28
K ₂ O	0.00	0.05	0.87	0.37	1.70	2.27	0.48	0.16	0.17	0.06	0.76	0.57	1.00	0.41	0.07	0.11
SO ₃	0.06	0.26	0.00	0.46	0.00	0.08	0.25	0.15	0.12	0.42	0.47	0.17	0.11	0.25	0.00	0.30
Total	96.51	97.60	96.79	96.42	96.70	96.36	99.50	96.11	97.55	95.42	98.09	99.02	96.41	98.99	97.22	98.54
Na ₂ O _{eq}	0.30		0.89		4.87		0.56		0.31		1.14		2.18		0.34	
Ca	3.01	2.99	2.00	1.98	3.00	3.13	2.00	2.05	3.03	2.96	2.03	2.03	3.00	2.96	2.03	2.01
Mg	2.89	2.89	1.91	1.94	2.53	2.62	1.90	2.03	2.94	2.84	1.89	1.97	2.65	2.83	2.01	1.98
Na	0.07	0.06	0.02	0.00	0.05	0.00	0.04		0.03	0.06	0.04	0.01	0.07			
K	0.03	0.01	0.04	0.02	0.30	0.36	0.04	0.01	0.01	0.03	0.05	0.03	0.22	0.09	0.02	0.02
Mn	0.00	0.00	0.03	0.01	0.10	0.14	0.02	0.01	0.01	0.00	0.03	0.02	0.06	0.02	0.00	0.01
Ti	0.01	0.00	0.00	0.01	0.00	0.00			0.01	0.01	0.01	0.00	0.00	0.02		
Fe	0.00	0.01	0.00	0.00	0.02	0.01			0.00	0.02	0.01	0.00	0.00	0.00		
Si	0.01	0.01							0.03	0.00						
Si	1.00	1.01	1.04	1.01	2.02	1.97	2.02	1.95	0.99	1.01	1.01	0.99	2.03	1.99	1.97	1.98
Al	0.97	0.97	0.95	0.98	0.32	0.37	0.18	0.19	0.95	0.98	0.93	0.95	0.27	0.27	0.19	0.07
Al	0.03	0.03	0.04	0.02	1.30	1.29	0.91	0.76	0.04	0.02	0.05	0.02	1.28	1.45	0.92	0.74
Fe			0.05	0.01	0.38	0.26	0.74	0.77			0.02	0.02	0.39	0.19	0.68	1.06
Mg					0.02	0.05	0.17	0.00					0.09	0.06	0.15	0.06
Mn							0.00	0.03							0.00	0.00
Ti							0.01	0.03							0.03	0.04
S	0.00	0.01	0.00	0.01	0.00	0.00	0.01	0.00	0.00	0.01	0.01	0.00	0.00	0.01	0.00	0.01
Cation	4.02	3.99	3.03	3.00	5.03	5.09	4.01	4.01	4.02	3.97	3.04	3.03	5.03	4.95	4.00	3.99
O	5.00	5.00	4.00	4.00	6.00	6.00	5.00	5.00	5.00	5.00	4.00	4.00	6.00	6.00	5.00	5.00
[Ca/Si]	2.97	2.98	2.01	1.99					3.00	2.88	2.03	2.06				
[Ca]/[Na+K]																
[Fe]/[Al+Fe]					0.23	0.17	0.45	0.50					0.24	0.12	0.42	0.59
Minimum clinker alkali	alite belite aluminate ferite Na ₂ O=0.29x0.6+0.49x0.2+3.57x0.1+0.35x0.1 = 0.66%								alite belite aluminate ferite Na ₂ O=0.23x0.65+0.71x0.15+1.72x0.05+0.29x0.15= 0.39%							
	K ₂ O=0.03x0.6+0.62x0.2+1.99x0.1+0.32x0.1= 0.37%								K ₂ O=0.03x0.65+0.62x0.15+1.99x0.05+0.32x0.15=0.23%							
	Na ₂ O _{eq} = 0.66+0.658x0.37 = 0.90%								Na ₂ O _{eq} = 0.39+0.658x0.23 = 0.53%							

thin section particle	Kingston experimental sidewalk					Concrete prism				C. microbar			Kentucky			
	Na		Nb	H	L	OPC		HAC		OPC	BFC		A			
	ASR gel	ASR gel	Mg-sil. gel	ASR gel	ASR gel	ASR gel	Calcite	ASR gel	Hydro t.alcite	ASR gel	ASR gel	glass	ASR gel	ASR gel	Bruc ite	glass
	1	1	4	2	3	1	1	1	1	1	1	1	2	4	4	4
dol ls	void	dol	void	dol ls	paste	paste	dol ls	dol	paste	paste	slag	dol ls	cht	dol ls	FA**	
SiO ₂	36.32	32.88	36.89	33.60	33.37	41.60	0.55	69.47	1.80	36.24	40.99	35.11	73.62	54.82	8.59	30.67
TiO ₂	0.06	0.47	0.00	0.38	0.29	0.00	0.23	0.08	0.38	0.14	0.50	0.68	0.01	0.10	0.00	1.96
Al ₂ O ₃	0.00	0.94	6.00	0.77	2.75	0.00	0.00	5.72	12.41	0.19	2.50	13.90	3.15	0.56	1.31	8.54
FeO *	0.30	0.28	2.29	0.00	1.55	0.16	0.00	1.09	1.58	0.59	0.00	0.08	0.19	0.47	1.17	6.79
MgO	0.00	0.00	20.01	0.00	0.18	0.00	0.00	0.10	16.85	0.00	0.00	5.14	0.00	0.00	36.44	8.34
CaO	28.39	32.88	1.97	38.86	28.59	25.51	49.55	0.83	3.79	31.22	29.51	42.07	5.52	15.54	2.69	40.16
Na ₂ O	0.45	0.46	0.00	0.12	0.13	0.97	0.25	0.06	0.00	2.11	0.76	0.11	0.28	2.64	0.04	0.04
K ₂ O	1.29	0.72	0.47	0.01	0.54	3.31	0.00	1.57	0.00	2.23	0.20	0.39	1.29	4.86	0.04	0.00
SO ₃	0.39	0.45	0.07	0.21	0.11	0.67	0.10	0.13	0.39	0.28	0.66	1.59	0.06	0.64	0.29	0.00
Total	67.20	63.64	67.70	73.94	67.51	72.22	50.67	79.06	37.20	73.00	75.11	99.06	84.12	79.62	50.58	96.49
[Ca/Si]	0.84	1.28		1.24	0.92	0.66		0.01		0.92	0.77		0.08	0.30		
[Ca]/[Na+K]	11.32	19.29		184.4	32.02	4.48		32.64		4.84	18.24		2.70	1.47		

* Total iron as FeO, **High-Ca fly ash

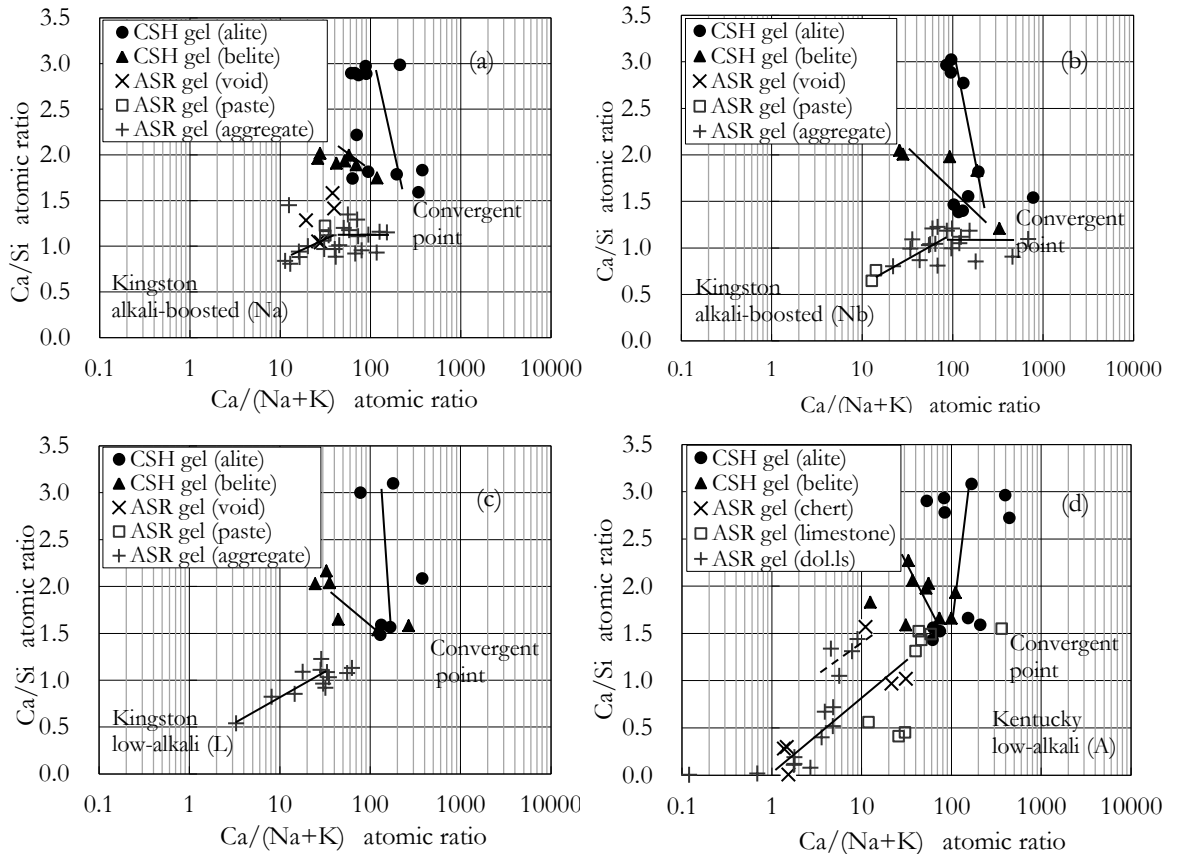


FIGURE 1: Compositional trends of ASR gel in ACR-affected concretes. (a) Alkali-boosted high-alkali section in Kingston studied in [2,3] (Na), (b) blind control (Nb), and (c) low-alkali section (L) in Kingston; (d) low-alkali concrete in Kentucky (A).

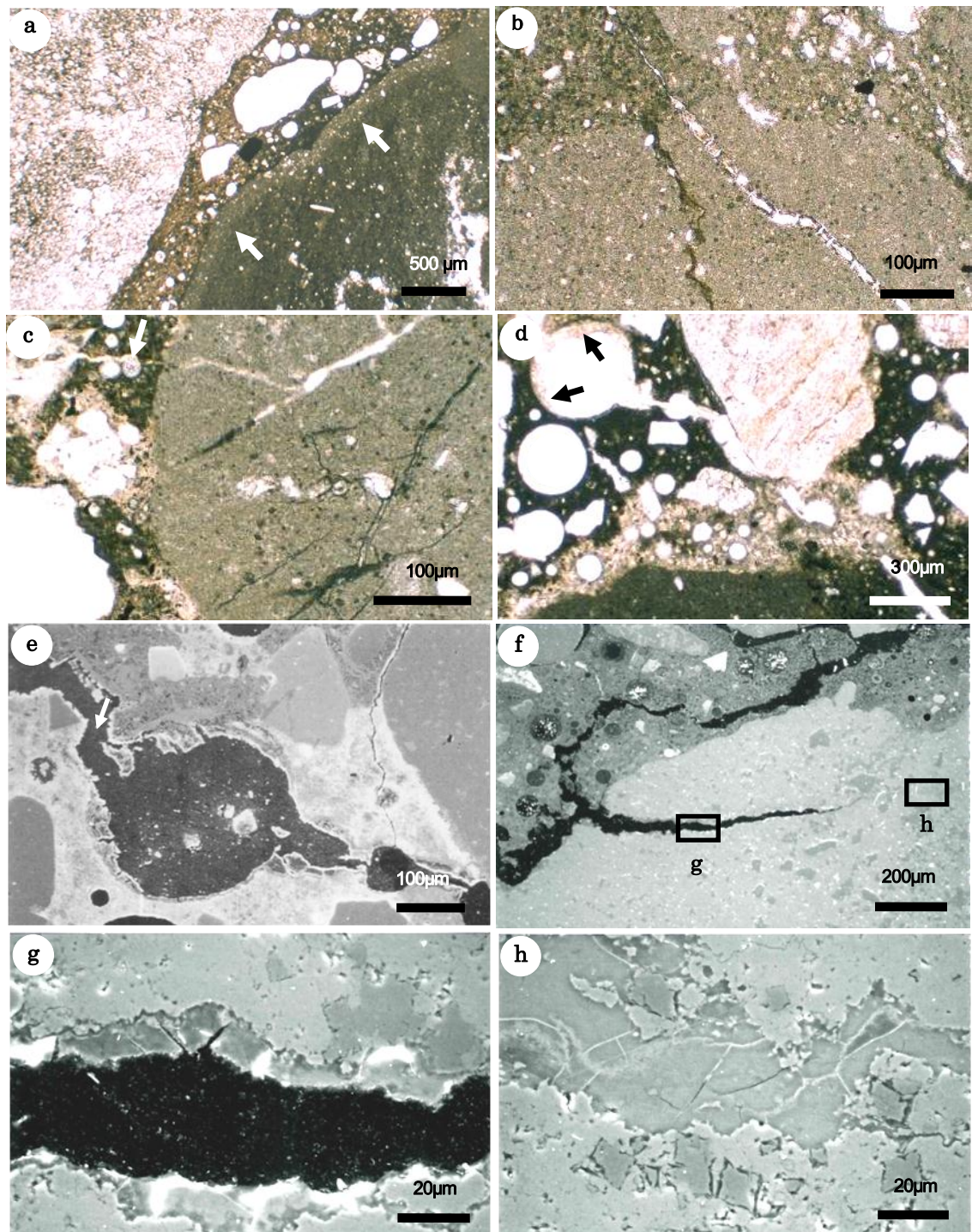


FIGURE 2: Kingston experimental sidewalk, Ontario: Alkali-boosted high-alkali concrete (high-alkali cement plus NaOH to $\text{Na}_2\text{O}_{\text{eq}}$ $3.88\text{kg}/\text{m}^3$, Na, Nb). (a)-(d): Sequence of crack formation: (a) Stage 1: rim formation (arrows); (b) Stage 2: internal cracking with ASR gel within aggregate; (c) Stage 3: cracking from aggregate into the cement paste, exuding ASR gel; (d),(e) Stage 4: ASR gel lining air void (arrows) along crack distant from aggregate; (f)-(h) ASR gel filling the crack that widens from the aggregate into cement paste (Stage 4).

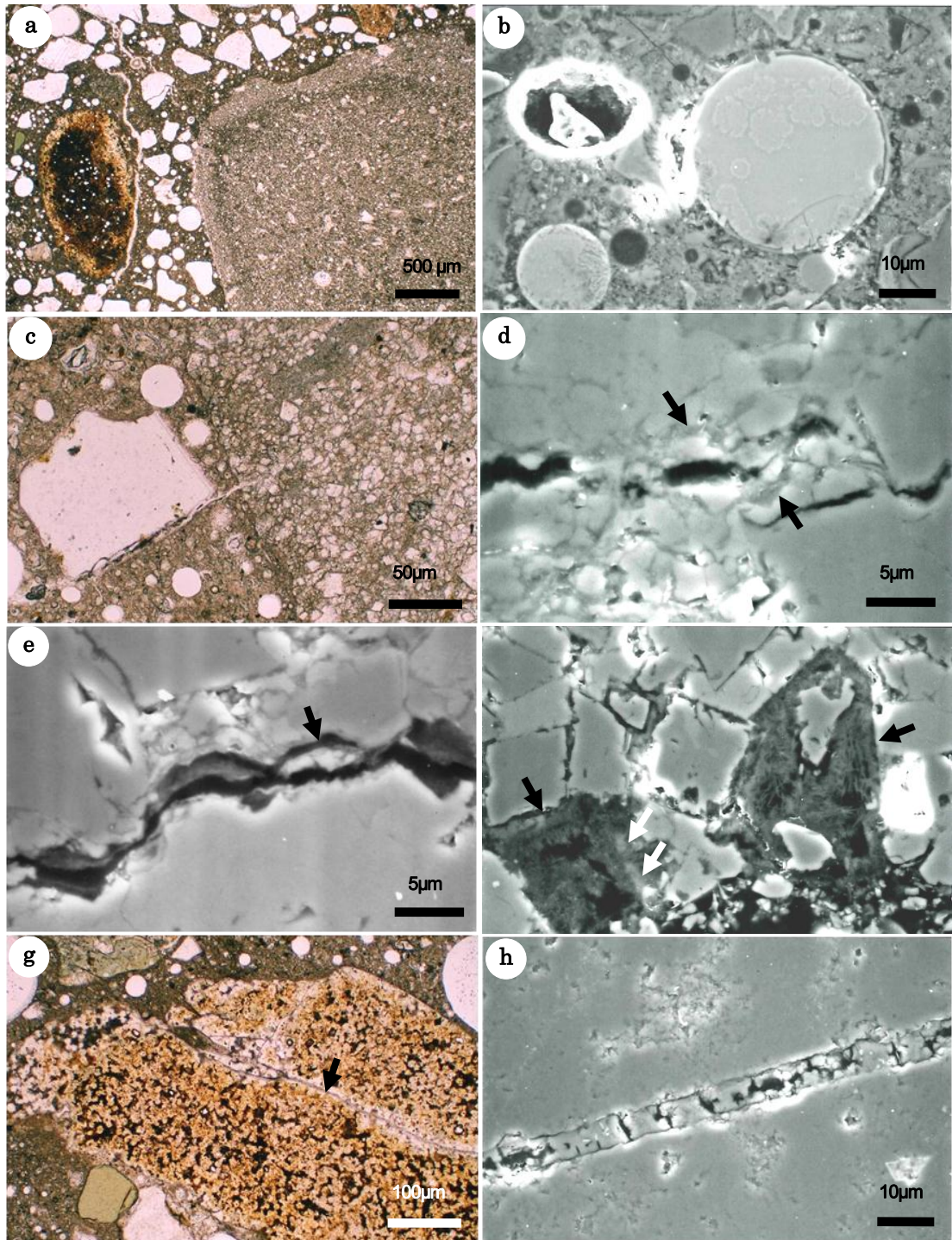


FIGURE 3: Concrete from a building in Kentucky, USA (with low-alkali cement, A): (a) Rim-formation of dolomitic limestone; (b) Unhydrated high-Ca flyash particles; (c) Crack running from dolomitic limestone into the cement paste; (d) Terminal of cracks filled with pools of ASR gel, the arrows point to gel; (e) ASR gel in the crack wearing out during sample preparation; (f) Pseudomorphs of brucite (black arrows) surrounding dolomite rhombohedra, intermixed with ASR gel (white arrows) (g),(h) Crack-filling ASR gel within reacted sand particle of chert

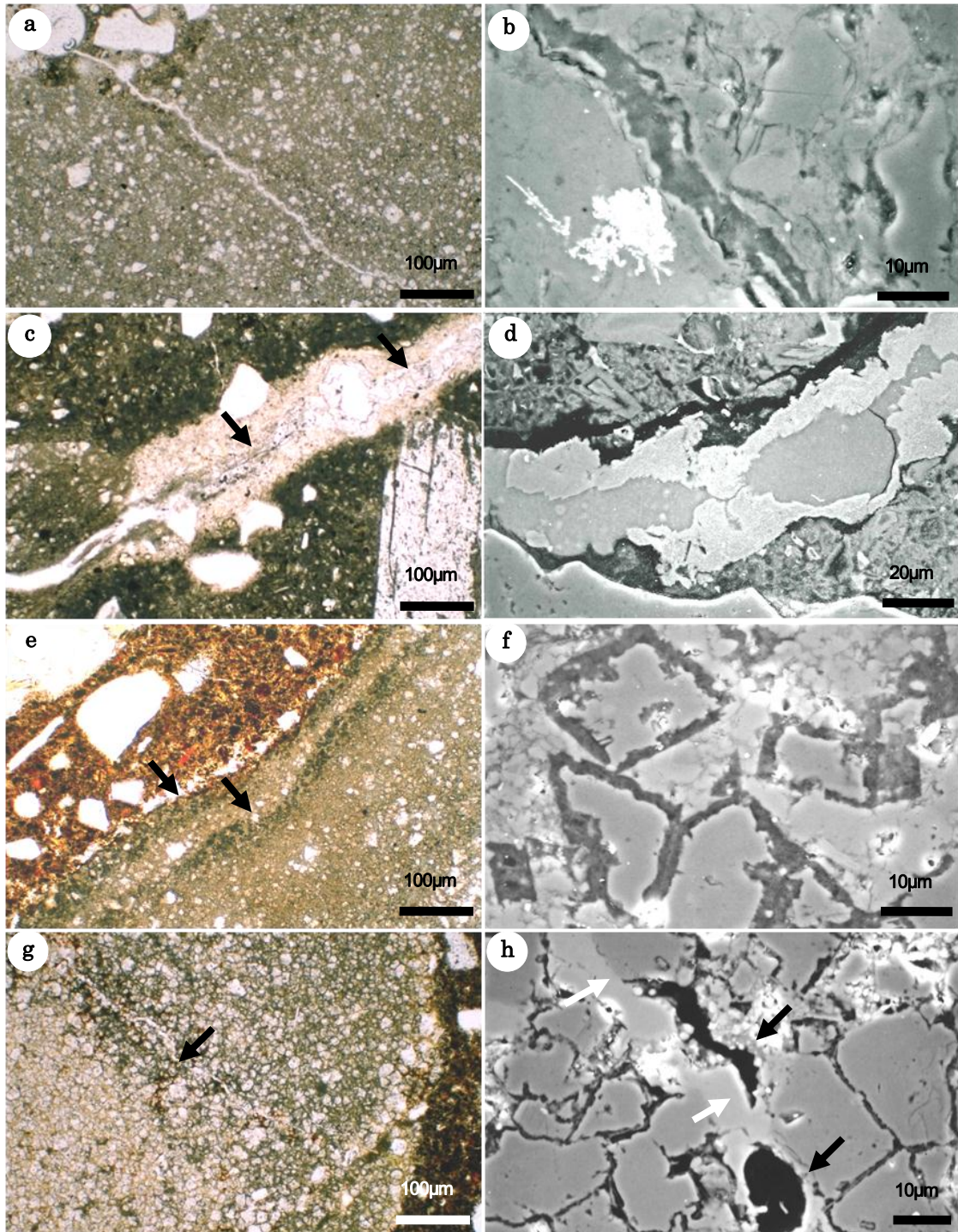


FIGURE 4: (a),(b) Kingston experimental sidewalk: Low-alkali concrete (with low-alkali cement Na_2O_{eq} $1.74\text{kg}/\text{m}^3$, I). (c),(d) Concrete prism with ordinary Portland cement (450 days) with radial expansion cracks filled with ASR gel (grey in SEM photograph (d)) later carbonated by calcite veins (bright in (d)). (e)-(h): Concrete prism with high-alumina cement (450 days); (e) Dedolomitization rims of aggregate (f) forming hydrotalcite rims on dolomite rhombohedra; (g) Dolomitic limestone with faint internal crack, (h) filled with bright calcite vein (white arrows) replacing a darker precursor ASR gel (black arrows).

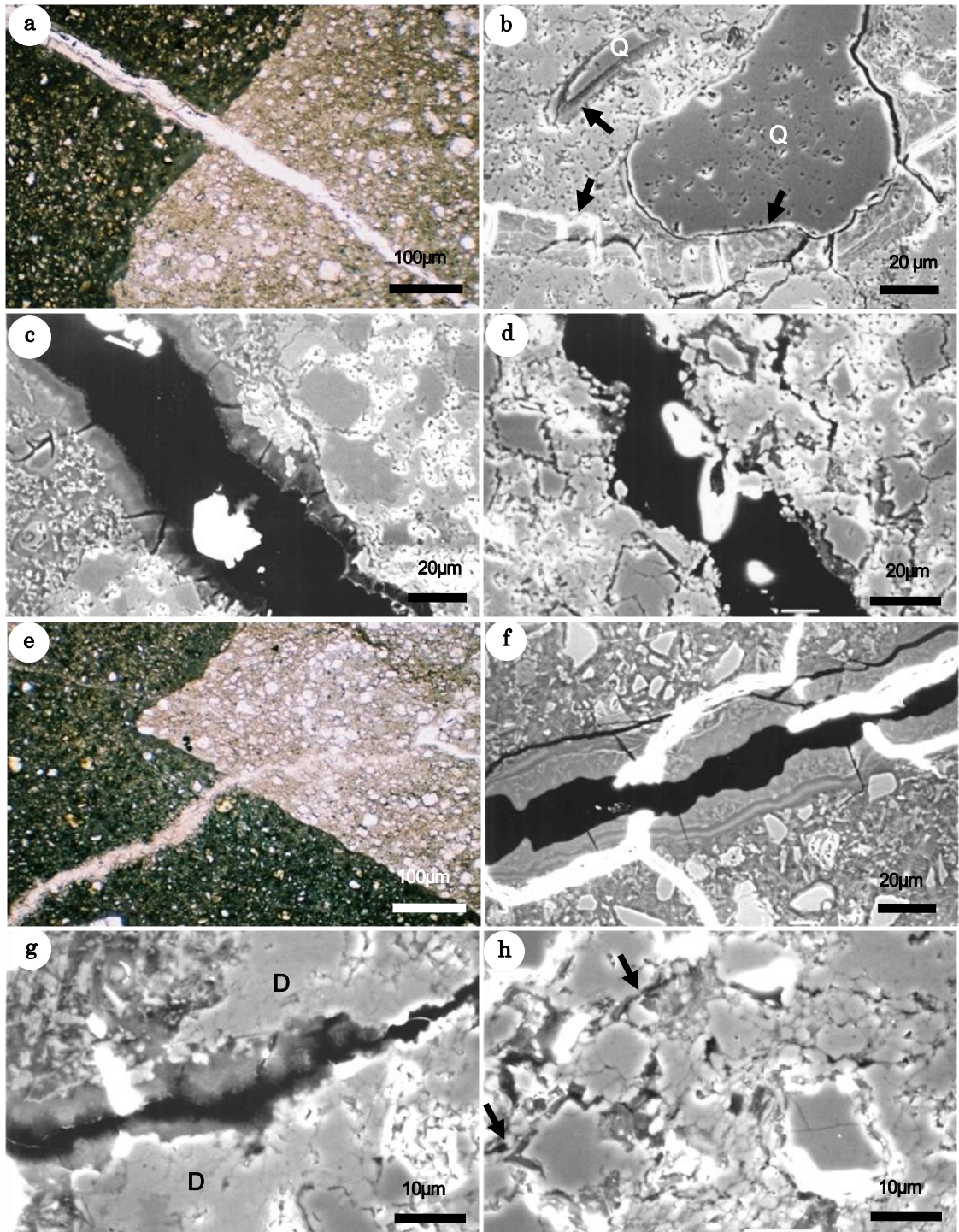


FIGURE 5: Concrete microbar (RILEM AAR-5) with cracks filled with ASR gel (28days in NaOH solution), thin sectioned after 2 years dry storage after testing: (a)-(d): Ordinary Portland cement (low-alkali): (a) Gel-filled crack; (b) Microcrystalline quartz (Q) converting to ASR gel; (c) Crack-lining ASR gel, (d) thinning out to the interior of the aggregate, with surface-decomposed dolomite rhombohedra along the crack. (e)-(h): Cement mixed with 50% blastfurnace slag. (e) Gel-filled crack; (f) Crack-lining ASR gel in cement paste; (g) ASR gel exuded to the mouth of the dolomitic limestone aggregate particle (D), (h) Dedolomitization along the terminating crack formed by ASR.